http://dx.doi.org/10.14311/asfe.2015.006

Applications of Structural Fire Engineering, 15-16 October 2015, Dubrovnik, Croatia

NUMERICAL ANALYSIS OF A COMPOSITE STEEL BOX GIRDER BRIDGE IN FIRE

Nicole Leo Braxtan,Qian Wang, Reeves Whitney, Gregory Koch

Manhattan College, Department of Civil Engineering, Riverdale, NY, USA

Abstract

Box girder bridges are becoming more common because of their ease of construction, pleasing appearance, and serviceability. Projects with curved configuration and long spans can especially benefit from these advantages. However, the industry lacks a wide range of research on multi-span steel box girder cross-sections and their response to fire events. This poses a major risk to unprotected steel bridges using a box girder design. This paper will discuss a mathematical approach to determining and classifying different failure modes of weathering steel box girder bridges subject to two fire cases. Due to the rapid increase of temperature in the thin steel members, the strength of the steel deteriorates quickly. Results show that different fire locations can greatly affect the forces that act on the individual members of the structure.

Keywords:steel box girder, composite bridges, fire, thermal analysis, finite element

1 INTRODUCTION

Fires that occur under a bridge pose a great risk to transportation infrastructure. Previous work by Garlock et al. (2014) discusses the current need for research in the topics of steel structures in fire. In addition, Wright et al. (2013) studies general fire hazards and how truck fires posea significant hazard to steel and concrete bridge structures. The work presented in this paper will touch on both the hazards and reactions of bridge structures to fire events. Using the finite element software Abaqus, a three span prototype bridges was modelled and analysed under fire loading. In order to capture both thermal and structural behaviour, sequential analyses were used to determine the response of the bridge during a hydrocarbon fire.

2 NUMERICAL MODELING

The straight steel box girder bridge used in this project was subject to sequential thermal and structural analyses using the commercially available finite element program Abaqus. The geometry of the bridge model follows the dimensions presented in the U.S. Department of Transportation FHWA Steel Bridge Design Handbook (FHWA 2012). Two symmetrical piers are located 57.15 meters from the abutments with the center span measuring 83.82 meters for a total of 198.12 meters long.Figure 1 shows a cross sectional view of the box girder, while Figure 3 illustrates the span conditions. This cross section is located above each of the interior piers. Transverse stiffeners were also present, located on both sides approximately every 5 meters and attached to the web.Cross sectional dimensions vary slightly along the length of the bridge. Variations occur in the top flange width and thickness, and in the bottom flange thickness. Also, the WT section is only located above the piers to resist bottom flange buckling in the negative moment regions. Full design dimensions and details can be seen in the FHWASteel Bridge Design Handbook (FHWA 2012).

The bridge model was created using both solid and shell elements in order to reduce the analysis run time while retaining an acceptable accuracy. For the thermal analysis, the model was constructed using 4 node, quadrilateral heat transfer shell elements (DS4), and 8-node, linear, solid, diffuse heat transfer elements (DC3D8). The structural model used 4-node structural shell elements (S4R), and 8-node, linear, solid, structural brick elements (C3D8R). An approximate mesh size of 0.10m produced a total of 601,303 nodes for the bridge. To achieve this level of work, state-of-art-

computer hardware and software was used including a workstation with a 10-Core Intel Xeon processor and 64 GB of RAM.

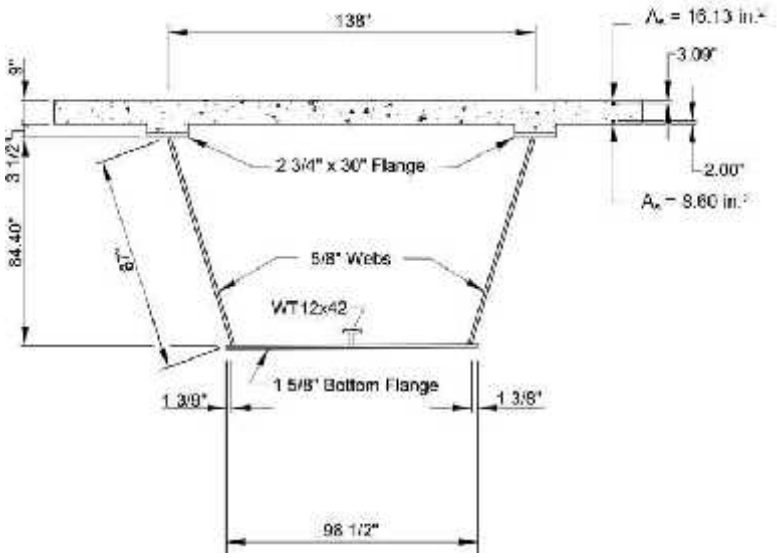

Fig. 1 Cross sectional dimensions of the weathering steel box girder bridge (FHWA 2012)

2.1 Material Properties

Temperature dependent thermal and structural material properties are assigned for the steel box girder and the concrete slab. Weathering steel was used for all steel elements. Thermal propertiesof weathering steel – including conductivity, specific heat, and thermal expansion– are referenced from Eurocode 3 (CEN 2005) and Cor-Ten (2014) product data. Structural properties of weathering steel are based on experimental testing performed by Labbouz (2014). Figure 2 shows the resulting temperature dependant stress-strain curves for the weathering steel. Weathering steel experiences a fairly steady decrease in yield strength between 20^{o}C and 700^{o}C. Traditional (non-weathering) steel maintainsyield strength until 400^{o}C and then experiences a rapid reduction.Siliceous concrete was used for the bridge slab. Both thermal and structural properties of siliceous concrete were referenced from Eurocode 2 (CEN 2005).

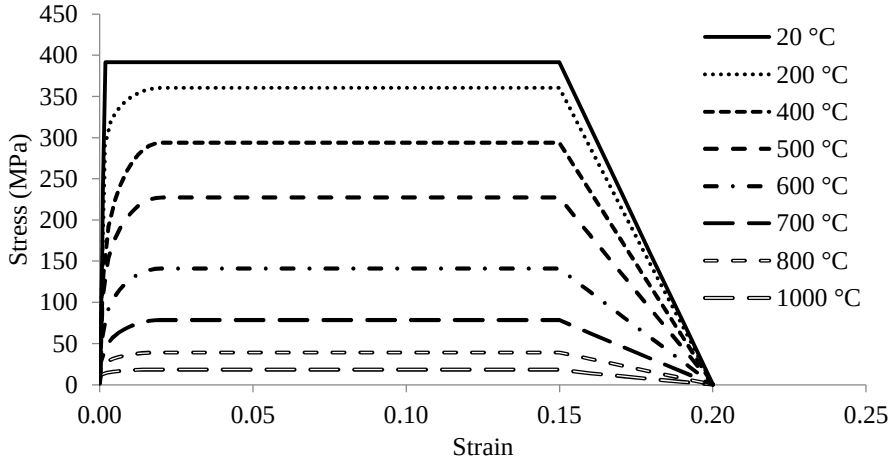

Fig. 2 Temperature dependent stress-strain curves for weathering steel

2.2 Thermal Loading andBoundary Conditions

Twofire scenarios were considered in order to observe the effect of fire location on the performance of the bridge girder. Figure 3 shows the locations of the fire applications. The first fire location was in the centre of the bridge, at point A. This location corresponds to the farthest distance that the fire

can be from any of the bridge supports. The second fire location is under one of the outer spans, directly adjacent to the inner bridge pier, at point B.

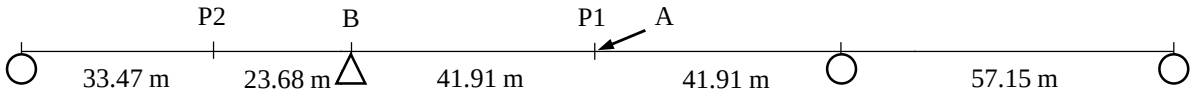

Fig.3 Schematic of bridge span, fire locations, and locations of maximum deflection.

The temperature history of the fire was assumed to follow the Eurocode 1 specification for hydrocarbon fire (CEN 2002), indicative of a vehicle fire underneath the bridge. For this analysis, a simulation was run for a 2 hour fire duration, with a maximum fire temperature of 1100^{o}C.A reduction in fire intensity was used along the length of the bridge. A fire gradient proposed by Alos-Moyaet al. (2014) was adapted to properly model a reduction in temperature in locations that are further from the fire. Figure 4 shows the distance dependent reduction curve.The reduction curve was adjusted into 5 meter sections that were applied to each segment (Alos-Moya et al. 2014).

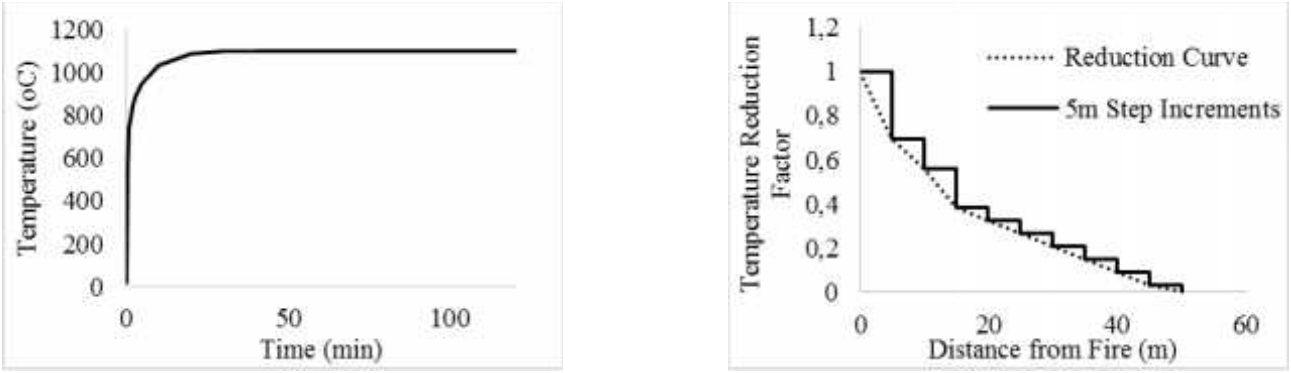

(a) (b)

Fig.4Thermal loading fire properties: (a) temperature of fire with respect to time; (b) reduction factor with respect to distance.

Thermal boundary conditions of convection and radiation were applied to the exposed bottom faces of the bridge through Abaqus interactions. A convection coefficient of 50 W/(m^{2}K)was specified for the hydrocarbon fire (CEN 2002). Radiation was defined using varying emissivityto account for the large depth of the box geometry. The bottom flange, web, top flange, and concrete slab have an emissivity of 0.7, 0.5, 0.3, and 0.3 respectively (Kodur et al. 2013). Stephan-Boltzmann constant was specified as 5.67 x 10^{-8} W/m^{2}K^4.These fire characteristics were applied to the surface of the bridge according to the distance reduction curve which resulted in a thermal temperature history for the steel and concrete. The temperature history was then applied to the entire model during the structural loading to capture the effects of the fire.

2.3 Structural Loading and Boundary Conditions

The structural analysis of the steel box girder bridge was performed considering two loading steps. First, the force of gravity was applied to the entire model simulating self-weight dead load over a 5 minute time period. Second, the temperature histories output from the thermal analysis were applied to the structural model. Figure 3 shows that there is only one pin support that will resistaxial translationbetween the outer and inner spans.

3 MODEL VALIDATION

A validation analysis was performed in order to show the applicability of the Abaqusfire modelling technique used in this study. An experimental test was conducted by Wainman et al. (1987) in

which a steel beam with a concrete slab was heated in a furnace while four point loads were applied to the beam. Loading was applied in a three-step process – first gravity loading, then temperature application, thenapplication offour concentrated 32.5 kN loads at quarter length intervals centred around the middle of the beam. Figure 5shows the final results from both the laboratory experiment and the Abaqus model. The Abaqus fire modelling results generally agreed with the experimental data.Further model validation information can be found in Braxtan et. al. (2015).

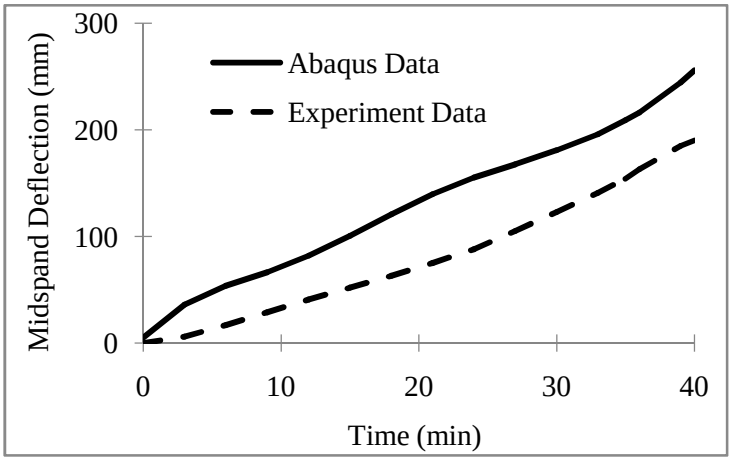

Fig. 5Beam deflection of Abaqus model and laboratory test.

4 NUMERICAL RESULTS AND ANALYSIS

Fire at location A, shown at the centre of bridge in Figure 3, results in a maximum deflection in the centre of the bridge at location P1. This is expected due to the symmetry of the geometry and loading. Once the fire step starts, there is a rapid increase in temperature of the steel members. This increase is more prominent in the web and bottom flange. The deflection of the bridge reaches a maximum at just over 10 minutes into the program time (5 minutes into the fire). The model ends at 14.1 total minutes (9.1 minutes of fire loading) when the model can no longer reach equilibrium and experiences instabilities.

Figure 6shows calculated moment demand to capacity ratio at the centrecross-section of the bridge based on AASHTO Bridge Design Specifications (AASHTO 2012).The moment capacity was calculated in accordance with Article 6.10.7.1.2 of AASHTO, with the demand obtained from applying the Strength IV load combination to the elastic bending moment diagram. Plastic moment capacity calculations were adjusted to incorporate reduced yield strength ofweathering steel based on average temperatures in the bottom flange, web, top flange, and slab. Once the fire begins at 5 minutes, the moment capacity of the bridge begins to decline. This decline correlates to the decreased yield strength of the weathering steel. The point at which the moment demand to capacity ratio exceeds one represents the time at which the bridge would be expected to fail based on the moment capacity limit state. This point was found to be 14.3 minutes.

For fire location B, the maximum deflection was seen at location P2, 23.68 meters to the left of support B (Fig. 3). The maximum deflection occurred at 17.1 minutes. At the location of the fire, there is minimal vertical deflection due to the adjacent support condition that restrains this movement. Figure 7 shows vertical deflection and the ratio of shear demand to capacity at point B. Nominal shear capacity of the section was calculated based on ASSHTO Bridge Design Specifications (AASHTO 2012). The calculations performed were adjusted based on the temperature dependant yield strength and stiffness of the weathering steel. It can be seen that the demand to capacity ratio approaches 1 shortly before the end of the simulation. Therefore, it is concluded that for a hydrocarbon fire applied at fire location B, the box girder is most likely to fail due to web shear capacity

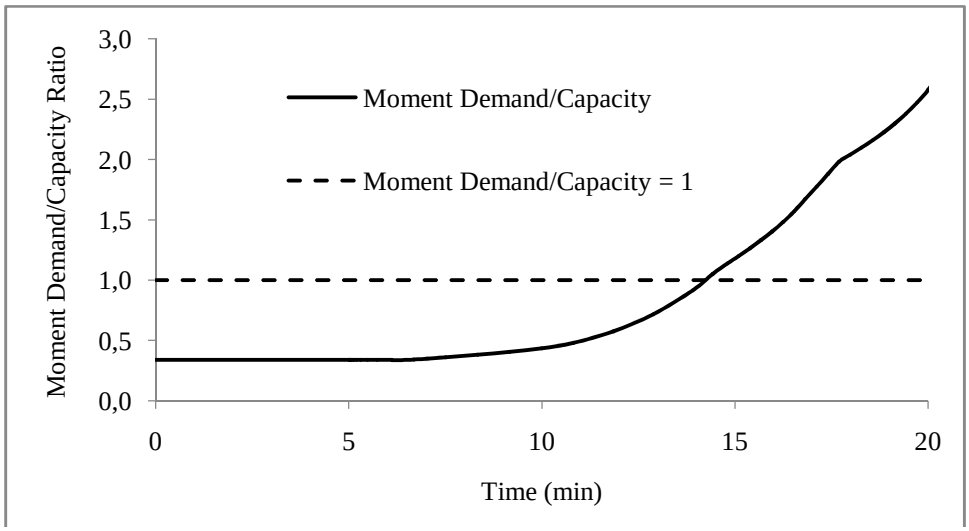

Fig.6 Momentdemand to capacity ratio over time

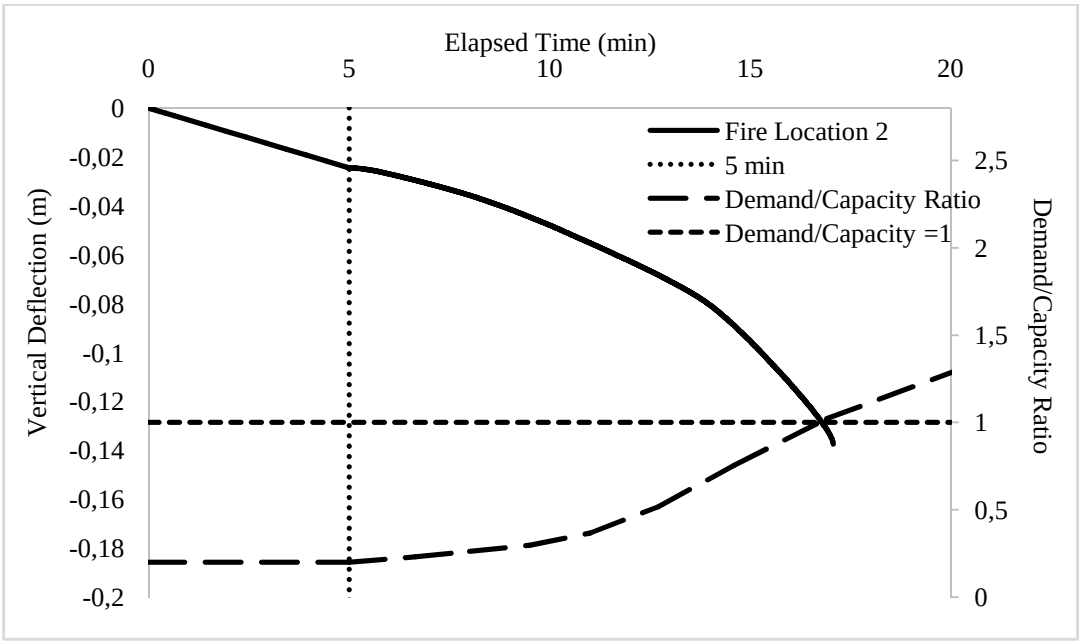

Fig.7Maximum deflection at point P2 and the shear demand/capacity ratio at point B

5 CONCLUSION

This research investigatedthermal and structural response of steel box girder bridges in fire.It was found that different fire locations could greatly affect the forces in the structure resulting in different failure modes of the bridge.

For a hydrocarbon fire applied to midspan of the bridge, maximum deflection occurs at midspan and moment demand is greatest at midspan. Results of the finite element model show good correlation with moment capacity as calculated by AASHTO and adjusted for temperature-dependent reductions in strength for both the steel girder and the concrete slab.

For a hydrocarbon fire applied adjacent to the support of the bridge, maximum deflection occurs at a distance away from the support and shear demand is greatest directly adjacent to the support. Results of the finite element model show good correlation with shear capacity as calculated by AASHTO and adjusted for temperature dependent reduction in strength and stiffness of the web. Additional research should be performed to investigate additional local issues in the bottom flange of the girder where temperatures are greatest, and the role of transverse stiffeners and web shear buckling at elevated temperatures.

ACKNOWLEDGEMENTS

The research presented in this paper was supported by the University Transportation Research Center (UTRC) through Grant #49198-28-26.

REFERENCES

AASHTO. (2012). LRFD Bridge Design Specifications, AASHTO, Washington, DC.

Alos-Moya, J., Paya-Zafortezo, I., Garlock, M.E.M., Loma-Ossorio, E., Schiffner, D., and Hospitaler, A. (2014). "Analysis of a Bridge Failure Due to Fire Using Computational Fluid Dynamics and Finite Element Models." *Engineering Structures*, 68, 96-110.

Braxtan, N.L., Whitney, R., Wang, Q., Koch, G. (2015) Preliminary investigation of composite steel box girder bridges in fire. Bridge Structures 11: pp. 105-114.

Cedeno, G., Varma, A., and Gore, J. (2011) Predicting the Standard Fire Behavior of Composite Steel Beams. Composite Construction in Steel and Concrete VI: pp. 642-656.

Cor-Ten™ Product Literature (2014), Nippon Steel & Sumitomo Metal Corporation. http://www.nssmc.com/product/catalog_download/pdf/A006en.pdf

European Committee for Standardization (CEN). (2002). "Actions on structures. Part 1.2: General action—Action on structures exposed to fire." Eurocode 1, Brussels, Belgium.

European Committee for Standardization (CEN). (2004). "Design of concrete structures. Part 1.2: General rules—Structural fire design." Eurocode 2, Brussels, Belgium.

European Committee for Standardization (CEN). (2005). "Design of steel structures. Part 1.2: General rules—Structural fire design." Eurocode 3, Brussels, Belgium

Garlock, M., Kruppa, J., Li, G-Q., and Xhao, B. (2014) "White Paper – Fire Behavior of Steel Structures." NIST. September 18, 2014.

FHWA. (2012). Design Example 4: Three-Span Continuous Straight Composite Steel Tub Girder Bridge. *Steel Bridge Design Handbook*. Publication No, FHWA-IF-12-052 – Vol. 24, Washington D.C.

Huang, Z., Burgess, I., and Plank, R. (1999). "The influence of shear connectors on the behavior of composite steel-framed buildings in fire." *Journal of Constructional Steel Research.* 51(3), 219-237.

ISO. (1975). "Fire resistance tests - elements of building construction." ISO 834, Geneva, Switzerland.

Kodur, V., Aziz, E., and Dwaikat, M. (2013). "Evaluating Fire Resistance of Steel Girders in Bridges." *J. Bridge Eng.*, 18(7), 633–643.

Kruppa, J. and Zhao, B. Fire Resistance of Composite Beams to Eurocode 4 Part 1.2. *J. Construct. Steel Res.* 1995; 33:51-69.

Labbouz, S. (2014). Evaluating weathering steel properties at elevated temperatures: The I-195 bridge fire case study.

Wainman, D.E., and Kirby, B.R. (1987). "Compendium of UK Standard Fire Test Data, Unprotected Structural Steel – 1," British Steel Corporation Ref. No. RS/RSC/S10328/1/98/B, Swinden Laboratories, Rotherdam.

Wang, A. (2012). "Numerical Investigation into Headed Shear Connectors under Fire." *J. Struct. Eng.*, 138(1), 118–122.

Wardhana, K. and Hadipriono, F. (2003). "Analysis of Recent Bridge Failures in the United States." *J. Perform. Constr. Facil.*, 17(3), 144–150.

Wright, W., Lattimer, B., Woodworth, M., Nahid, M., and Sotelino, E. (2013). "Highway Bridge Fire Hazard Assesment, Draft Final Report." Virginia Polytechnic Institute and State University. TRB Project No. 12-85. Blacksburg, VA.